# LANGMUIR

pubs.acs.org/Langmuir Article

# Reconfigurable Pickering Emulsions with Functionalized Carbon Nanotubes

Quynh P. Ngo, Maggie He, Alberto Concellón, Kosuke Yoshinaga, Shao-Xiong Lennon Luo, Nouf Aljabri, and Timothy M. Swager\*



Cite This: Langmuir 2021, 37, 8204-8211



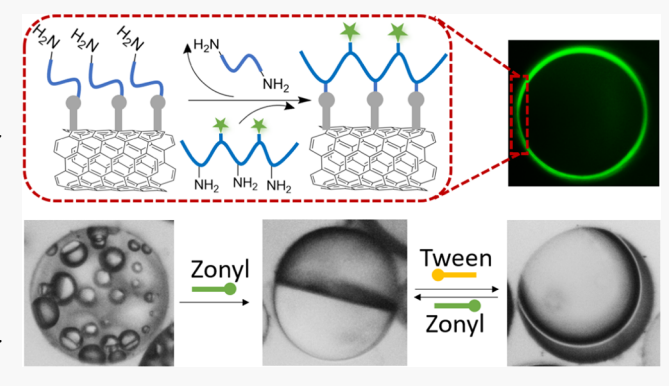
**ACCESS** 

III Metrics & More

Article Recommendations

Supporting Information

ABSTRACT: Pickering emulsions (PEs) achieve interfacial stabilization by colloidal particle surfactants and are commonly used in food, cosmetics, and pharmaceuticals. Carbon nanotubes (CNTs) have recently been used as stabilizing materials to create dynamic single emulsions. In this study, we used the formation of Meisenheimer complexes on functionalized CNTs to fabricate complex biphasic emulsions containing hydrocarbons (HCs) and fluorocarbons (FCs). The reversible nature of Meisenheimer complex formation allows for further functionalization at the droplet—water interface. The strong affinity of fluorofluorescent perylene bisimide (F-PBI) to the CNTs was used to enhance the assembly of CNTs on the FC—water interface. The combination of different concentrations of the functionalized CNTs and the pelene



additive enables predictable complex emulsion morphologies. Reversible morphology reconfiguration was explored with the addition of molecular surfactants. Our results show that the interfacial properties of functionalized CNTs have considerable utility in the fabrication of complex dynamic emulsions.

#### **■ INTRODUCTION**

Pickering emulsions (PEs) are widely used in food,1 cosmetics,<sup>2</sup> and pharmaceutical<sup>3</sup> formulations. The wide utilization stems from the fact that PEs achieve high stability as a result of the stronger adsorption of the particles at the interface as compared to small-molecule surfactants.<sup>4,5</sup> However, the stability of PEs generally leads to static systems that do not respond to small environmental changes and have limited utility in biosensing<sup>6-8</sup> and dynamic optics.<sup>9</sup> Another drawback of many PEs is a lack of interfacial chemical tunability. PEs are generally prepared from functionalized particles, and additional post-emulsification functionalization of the colloidal particles is challenging. This aspect severely limits the addition of functional groups that can enable more complex sensing conditions such as biosensing. <sup>6,7,10</sup> As a result, colloidal particles with functional groups that display dynamic covalent functionalization are desired in order to create emulsion interfaces with dynamic/expanded functionality.

Carbon nanotubes (CNTs) have previously been used as stabilizing colloidal particles in PEs. 11-13 CNTs are, in general, very hydrophobic and require modification to be more hydrophilic in order to stabilize the oil—water interface. Non-covalent functionalization has been investigated, but has limited stability when the functional groups can easily desorb from CNTs. 14,15 This approach can also produce inconsistent outcomes as a result of the dynamic degree of CNT

functionalizations that vary with conditions, organizations, and concentrations. Covalent sidewall functionalization of CNTs by oxidative methods to introduce hydroxyls or carboxylates has also been investigated; 12,16,17 however, these methods are highly non-specific in terms of the structures formed.

To address these limitations, we have developed functional CNTs that display dynamic covalent equilibria to produce tunable complex PEs. Specifically, we have functionalized the CNT surfaces with 3,5-dinitrophenyl groups that form Meisenheimer complexes (MCs) with primary amines. <sup>18</sup> MCs display reversible equilibria such that the interfacial characteristics of an as-formed PE can be dynamically changed in situ. <sup>18,19</sup> By controlling the concentration of CNTs and interfacial assembly of CNTs at multiple water—oil interfaces, different morphologies of double emulsions are obtained. Addition of molecular surfactant changes the morphologies reversibly.

Received: April 1, 2021 Revised: June 15, 2021 Published: June 30, 2021





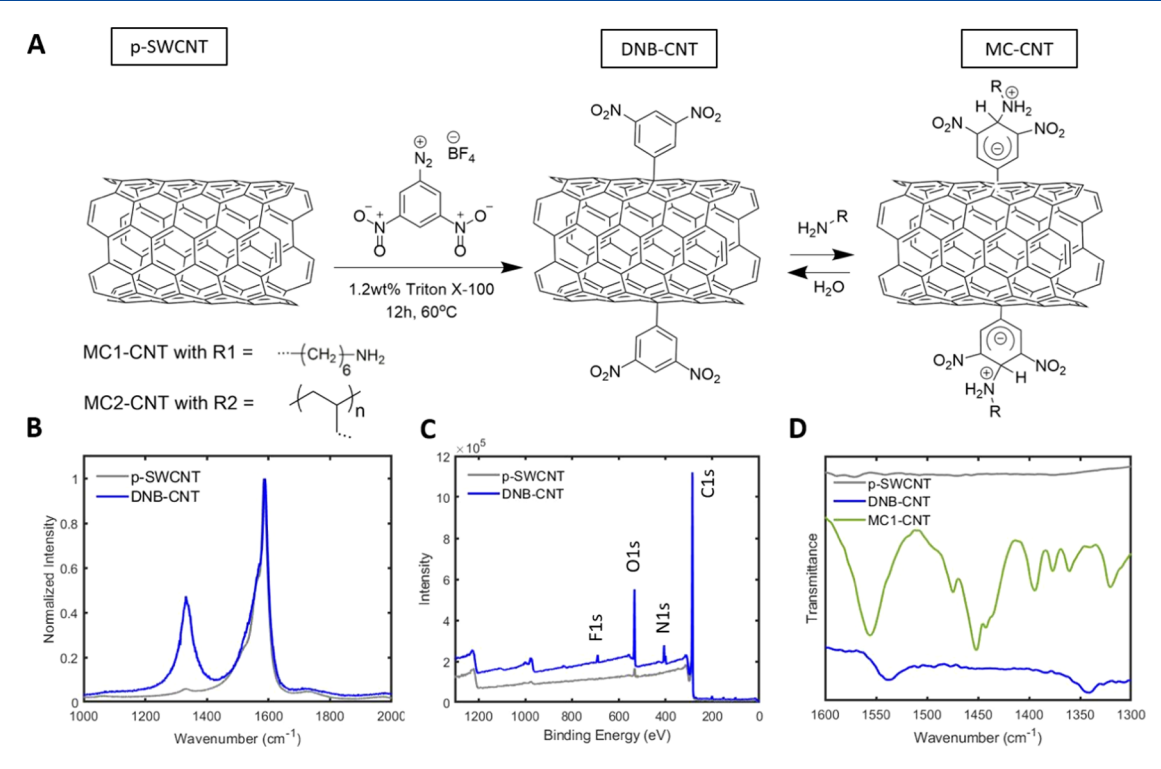


Figure 1. (A) Synthesis strategy of MC-CNTs. MC1-CNT is a functionalized SWCNT that has formed an MC with hexamethylenediamine (HMDA) and MC2-CNT is a functionalized SWCNT in an MC with poly(allylamine). (B) Raman spectra of the functionalized SWCNT, (C) XPS spectra of the functionalized SWCNT, and (D) attenuated total reflectance-Fourier transform infrared (ATR-FTIR) spectra of p-SWCNT, DNB-CNT, and MC1-CNT.

#### RESULTS AND DISCUSSION

Functionalized Carbon Nanotubes. Functionalization of the single-walled CNTs (SWCNTs) is accomplished by reaction with 3,5-dinitrobenzenediazonium salt, which reacts via a phenyl radical reductively generated in situ. The resulting 3,5-dinitrophenyl functionalized SWCNTs (DNB-CNTs) react with primary amines to form Meisenheimer complex functionalized SWCNTs (MC-CNTs) (Figure 1A). 18 Figure 1B shows the Raman spectra of pristine-SWCNTs (p-SWCNTs) and DNB-CNTs. The intensity of the D-band is a measure of sp<sup>3</sup> hybridization defects that result from the covalent functionalization of the graphene walls.<sup>20</sup> Using the starting p-SWCNTs as reference  $(A_D/A_G = 0.06)$ , our DNB-CNTs show a large increase in the intensity of the D-band  $(A_D/A_G = 0.47)$ , thereby suggesting extensive functionalization. Quantification of the functionalization was accomplished using X-ray photoelectron spectroscopy (XPS). From Figure 1C, we can see that our DNB-CNTs contained F, O, and N, with N and O present at much higher concentrations than p-SWCNTs. Fluorine, present at an extremely small amount (less than 0.5 atom %), is introduced from the BF<sub>4</sub> - counterion. The highresolution XPS scan of N1s reveals two distinct binding energy peaks that are assigned to N-C and N-O bonds associated with the nitro groups (Figure 1).<sup>21</sup> Based on the atomic percentages obtained from XPS (Table S1), the number of functional groups per 100 carbons is 2.5.

To further confirm the chemical identity of the covalent functional groups and the MC formation, ATR-FTIR was performed (Figure 1D). The DNB-CNTs show the expected distinct nitro stretching bands at 1537 and 1344 cm<sup>-1</sup>. These nitro stretches are shifted to 1473 and 1321 cm<sup>-1</sup>, respectively, when MCs are formed.<sup>18</sup> The shift to the lower energy of the

nitro stretching bands is consistent with the negative charge that is distributed within the dinitrophenyl system in the MC.<sup>18</sup> There are other signals detected from the MC1-CNT that confirm the presence of the small-molecule amine associated with the MCs (Figure S5). Upon extended washing the MC1-CNTs with water, the nitro stretches shift back to 1537 and 1344 cm<sup>-1</sup>, confirming the reversibility of the MC formation with HMDA. Polymeric amines, such as poly-(allylamine), were used to form MCs with DNB-CNTs (ATR-FITR shown in Figures S7 and S8). The MC nitro stretching bands at 1484 and 1306 cm<sup>-1</sup> of the MC2-CNTs do not change after washing with water, indicating that the multivalent nature of the polymeric amines prevents dissociation.<sup>22</sup>

Meisenheimer Complex Formation at the Oil-Water **Interface.** We began with an evaluation of the potential of MC-functionalized CNTs to stabilize single oil-in-water emulsions. MC1-CNTs are better at stabilizing CNTs and do not form aggregates in water. The MC1-CNTs assemble more evenly at the droplet surface. MC2-CNTs form large aggregates in water that do not stabilize the oil-water interface. MC2-CNTs stabilized the droplets and thereby were fabricated by leveraging the reversibility of MC formation through an in situ modification of the MC1-CNT-stabilized droplets. Figure 2A shows the process wherein by exchanging the aqueous amine solution, MC1 transforms to MC2 at the interface of the droplets. Figure 2B shows an optical microscope image of HFE7500 droplets stabilized with MC2-CNT. Upon washing the droplets with pure amine-free water, the MC1-CNT-stabilized droplets quickly aggregate without coalescing, while MC2-CNT-stabilized droplets remain stable without aggregation (Figure S11). Washing the MC1-CNT droplets with pure water removes the HMDA and lowers the effectiveness of the CNT surfactants. In contrast,

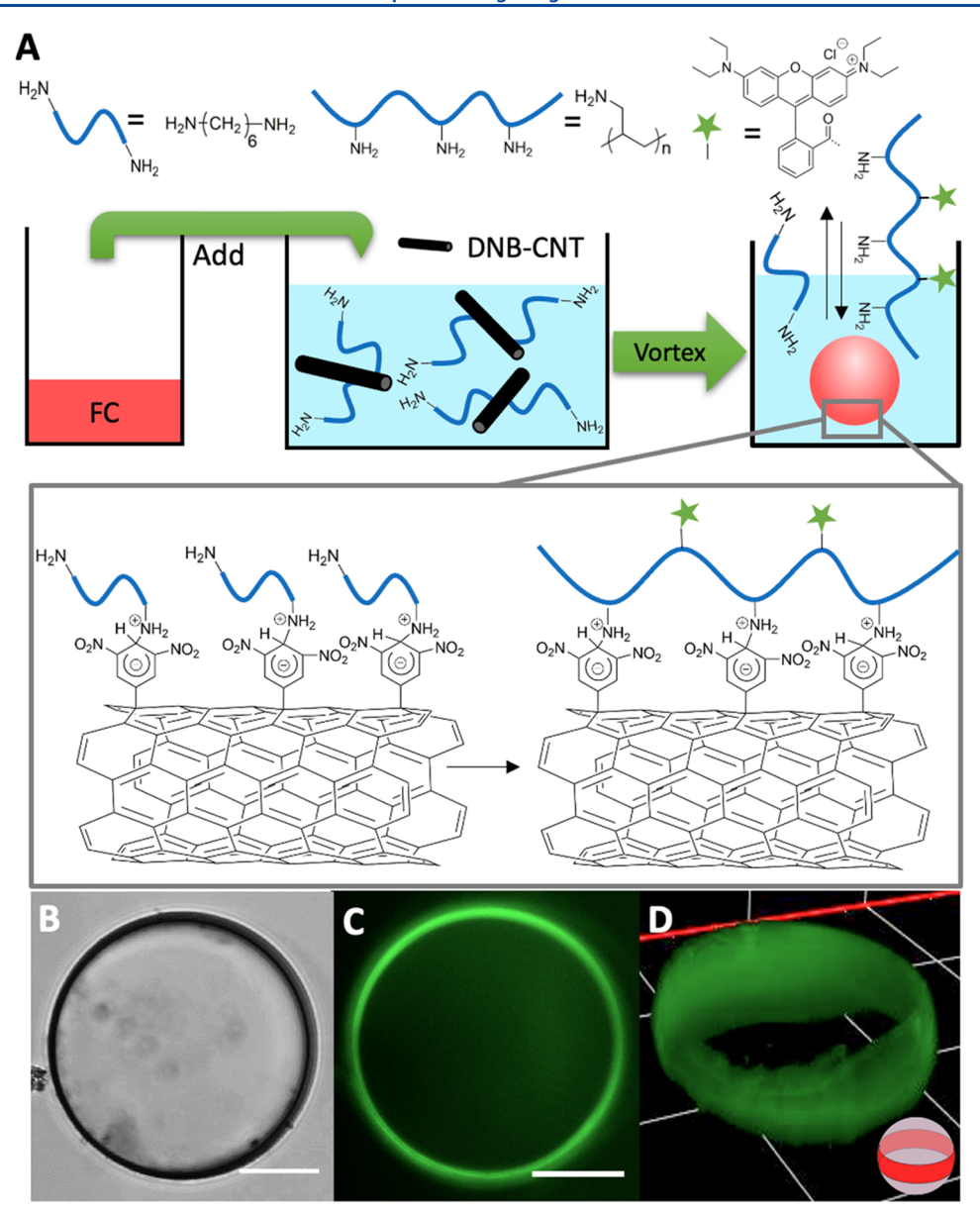


Figure 2. (A) Fabrication scheme for the formation of fluorocarbon (FC) single emulsions with MC1-CNT and amine exchange occurring when the HMDA solution is replaced with PAA-RB solution. (B) Optical image of an oil-in-water droplet stabilized by MC2-CNT. (C) Top-view fluorescence image of the droplets. (D) Z-stack image showing the localization of the emission at the droplet's oil—water interface. Scale bar = 50  $\mu$ m.

the poly(allylamine) in MC2-CNT-stabilized droplets is irreversibly connected to the functional CNTs and maintains a barrier for the interdroplet association. In the absence of the MCs, the strong interaction between CNTs causes the droplets to stick to each other, which eventually leads to coalescence.<sup>23</sup> To confirm the poly(allylamine) at the interface of the droplets, a fluorescent label, PAA-RB, was used in MC2-CNT. Figure 2C shows a fluorescent image of HFE7500 droplets stabilized with MC2-CNTs, and a confocal Z-scan reveals that Rhodamine B is localized to the droplet surface and is not distributed to the inside of the droplet (Figure 2D).

**Double Emulsions.** Pickering double emulsions were fabricated with MC1-CNTs, wherein each droplet contained a 1:1 ratio of hydrocarbon (HC) and fluorocarbon (FC) oils. We used diethylbenzene (DEB) and HFE7500 as HC and FC oils, respectively. The immiscibility of fluorocarbons with hydrocarbons translates to their surface characteristics, and

additional functionality is needed to create a thermodynamic driving force to competitively localize functional CNTs to the FC-W interface in the presence of an HC-W interface. We hypothesized that molecules with strong interactions with CNTs, such as a perylene<sup>24-28</sup> with fluorous character, could be used for CNT assembly at the FC-W interface. In this context, the fluorocarbon soluble perylene, fluorofluorescent perylene bisimide (F-PBI),<sup>29</sup> was added to FC oil for the controlled formation of HC-FC double emulsions, as shown in Figure 3.

The morphologies of the double emulsion droplets were investigated as a function of the concentrations of CNTs and F-PBI. At a fixed F-PBI concentration of 10 mg/mL in the FC phase and varying concentrations of CNTs from 10 to 20 mg/L in the bulk water phase (Figure 4A), the morphologies of droplets display a symmetric Janus structure. This structure indicates that the interfacial tensions at the FC–W and HC–

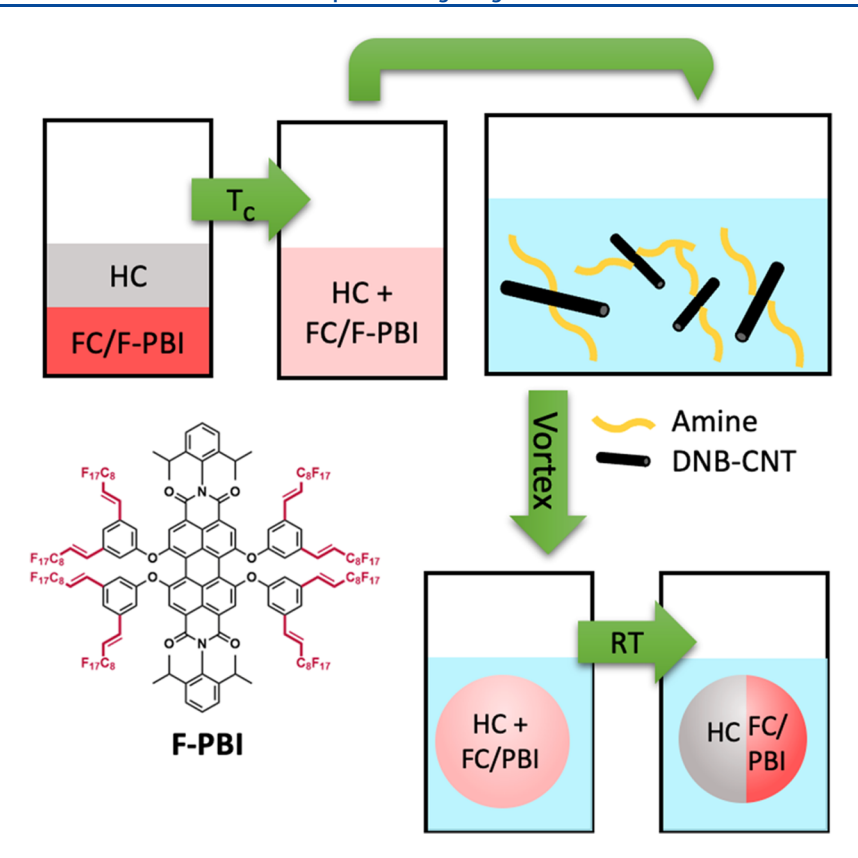


Figure 3. Fabrication scheme for Pickering double emulsions.

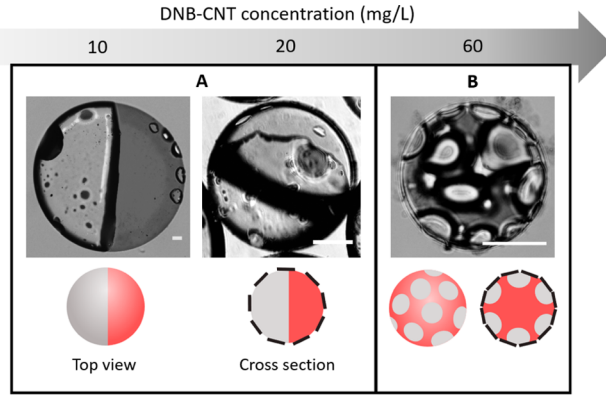
W interfaces are approximately equal.<sup>30</sup> The average size of the droplets shows a significant decrease as CNT concentration increases (Figure S9), which is to be expected with a higher surfactant-to-oil ratio. 11 At higher CNT concentrations (60 mg/L), we generated droplets that contain multiple HC domains as smaller domains within the FC phase (mHC-FC/ W) (Figure 4B). We hypothesized that high CNT concentrations give a densely rigid interfacial network, which prevents the coalescence of HC domains upon phase separation when the temperature is reduced below the  $T_c$  (which is 42 °C for DEB and HFE7500 oils). Figure 4B shows this structure and similar morphologies are often transiently observed during the phase separation of the oil phases of the droplets upon cooling (Figure S12). However, with small-molecule surfactants, these droplets quickly convert to more thermodynamically stable Janus structures. With the higher concentration of CNTs, the temperature-triggered phase separation process produces kinetically trapped multi-droplet morphologies.

In another series of experiments, the CNT's concentration was fixed at 60 mg/L, and the F-PBI concentration was varied. In the absence of F-PBI in the FC oil, an FC-in-HC-in-W (FC/HC/W) double-emulsion morphology is generated (Figure 4C), which indicates that CNTs prefer to assemble at the HC-W interface over the FC-W interface. When the F-PBI concentration is increased from 10 to 50 mg/mL, the morphology changes from an mHC-FC/W toward an HC-in-FC-in-W (HC/FC/W) morphology (Figure 4D,E). We observed that the FC-W interfacial area increases significantly when F-PBI's concentration increases from 0 to 10 mg/mL. The strong interactions of F-PBI with CNTs direct assembly at the FC-W interface. These interfaces behave as barriers against phase separation, and the droplet's interface kinetically traps the HC in smaller domains. When the concentration of

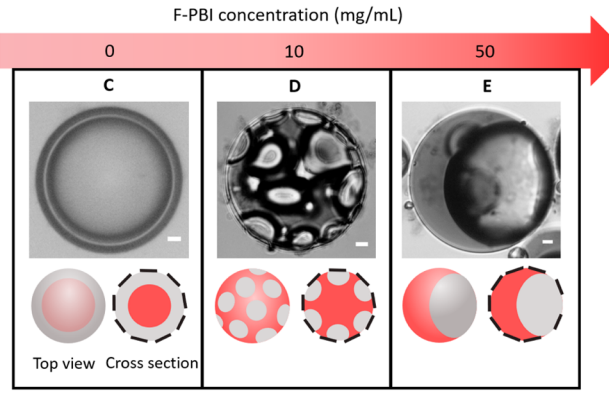
F-PBI is increased to 50 mg/mL, more CNTs are adsorbed onto the FC-W interface. In addition, molecules with a similar structure to our F-PBI have been shown to reduce the interfacial tensions between the HC-FC phases,<sup>30</sup> and hence this additive can also stabilize the multidomain structure by stabilizing the expanded HC-FC interfacial area.

We performed similar experiments with a fixed concentration of MC1-CNTs at a reduced concentration of 10 mg/L and varying F-PBI concentrations. As expected, in the absence of F-PBI, the droplets display the FC/HC/W morphology (Figure 4F). As the F-PBI concentration increases from 1 to 10 g/L, the morphology gradually changes from a partial Janus (Figure 4G) to a symmetric Janus morphology (Figure 4H). Similar to the other experiments, a higher concentration of F-PBI facilitates more adsorption of CNTs to the FC−W interface and increases its area. However, the mHC-FC/W morphology is not observed at higher F-PBI concentrations (≥10 mg/mL), as shown in Figure 4D. Apparently, the CNT concentration is insufficient to form the static interfacial structures that kinetically trap this phase.

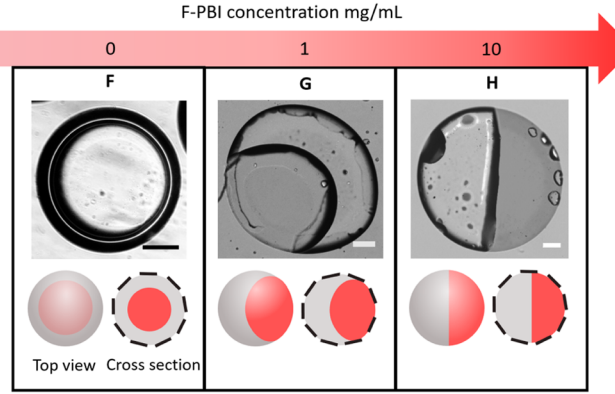
Dynamic Double Emulsions. After obtaining the complex double emulsions stabilized solely by MC-CNTs, we endeavored to see if the droplet morphologies can be dynamically modified by the addition of other surfactants. In these studies, we made use of Zonyl FS-300 (Zonyl), a water-soluble surfactant for the FC phase, and Tween 20 (Tween), a water-soluble surfactant for the HC phase. For droplets stabilized by 60 mg/L of MC1-CNTs or MC2-CNTs in the continuous water phase, but lacking F-PBI, the morphology changed from FC/HC/W to a Janus structure upon adjusting the Zonyl concentration in the water to 1 wt % (Figure 5A). This change in morphology could be reversed when the aqueous phase concentration of Tween was 1 wt %. All of the



10 mg/mL F-PBI



60 mg/L of DNB-CNTs



10 mg/L of DNB-CNTs

Figure 4. (A, B) Morphology of the complex fluorocarbon/hydrocarbon droplets at increasing concentrations of MC1-CNTs (10–60 mg/L) with a constant F-PBI concentration of 10 mg/mL. Scale bar = 50  $\mu$ m. (C–E) Morphologies of the droplets as a function of increasing F-PBI concentration (0–50 g/L) with a constant MC1-CNT concentration of 60 mg/L. Scale bar = 10  $\mu$ m. (F–H) Morphologies of the droplets as a function of increasing F-PBI concentration (0–50 mg/mL) with a lower constant MC1-CNT concentration of 10 mg/L. Scale bar = 100  $\mu$ m.

changes in morphology occur within 5 min of adding the molecular surfactants. The power of the MC-CNT surfactants is revealed by the fact that even with a large excess of Zonyl (1 wt %), the Janus structure persists. In the case of molecular surfactants, large Zonyl concentrations can displace the organic phase surfactants and generate a HC/FC/W morphology. To visualize where the CNTs were located before and after the morphology change, we used the fluorescent PAA-RB-labeled MC2-CNTs to stabilize the FC/HC/W droplets. The

fluorescence images in Figure 5A reveal that CNTs covered the entire droplet surface. After switching the continuous aqueous phase to contain 1 wt % Zonyl, only the HC hemisphere is covered with CNTs. Even at higher concentrations of Zonyl, we are unable to produce HC/FC/W droplets because the CNTs are tightly bound to the HC–W interface and act as a barrier against further morphology change.

When F-PBI is present in the FC phase, another dynamic behavior is observed. Images of droplets made with 60 mg/L of MC1-CNTs in the water phase and 1 mg/mL of F-PBI in the FC phase are shown in Figure 5B. The mHC-FC/W morphology changes to a Janus structure when the aqueous phase is adjusted to 1 wt % of Zonyl. Subsequent addition of Tween (1 wt % in water) changes the morphology to where the HC almost encapsulates the FC phase. The last two morphologies are reversible by adding Zonyl (1 wt %) or Tween (1 wt %). The addition of organic surfactant speeds up the phase separation process of the FC and HC oils and releases the droplets from the kinetically trapped thermodynamically unstable polydomain morphology to a more stable morphology. The systems that contained F-PBI in the FC phase could not be driven to the states wherein one oil is encapsulated by the other. This is because the CNTs are strongly and irreversibly bound to both the FC-W and HC-W interfaces.

The amount of CNTs adsorbed at the interface controls the droplets' morphology when excess organic surfactants are added. In Figure 6A, double-emulsion droplets made with 10 mg/mL of F-PBI are exposed to excess (>1 wt %) Zonyl. As the concentration of the CNTs increases, the  $\Theta_{\rm F}$  increases, which reflects an increasing surface area of the HC–W interface. This is the result of more CNTs assembling at the HC–W interface. In Figure 6B, double-emulsion droplets made with 60 mg/L of CNTs are exposed to excess (>1 wt %) Tween. Similar to Figure 6A, as the concentration of F-PBI increases, so too does the  $\Theta_{\rm H}$  as a consequence of a larger FC–W interfacial area. Here again, the F-PBI causes CNTs to assemble at the W–FC interface.

#### CONCLUSIONS

In summary, using MC-functionalized CNTs, we have demonstrated a one-step process method to fabricate complex Pickering emulsions. The dynamic MC chemistry at the interface allows for the interfacial reactions with the amines in the aqueous solution. The nature of the amine molecules/ polymers controlled the stability of the droplets, with the multivalent polymeric amines displaying superior MC stability. Methods that predictably produced different morphologies for double emulsions by varying the CNT and F-PBI concentrations were developed. Increasing the CNT and F-PBI concentrations led to a gradual change in morphology ranging from a kinetically stable morphology (Janus or FC/HC/W) to kinetically trapped and unstable (mHC-FC/W) multidomain morphologies. In the latter case, the rigid network of highconcentration CNTs acted as the barrier for the consolidation of the phases within a given droplet. F-PBI facilitated the adsorption of CNTs to the W-FC interface. Higher concentrations of F-PBI resulted in a higher amount of CNTs adsorbing to the interface, which led to a larger FC-W interfacial area. The CNT-stabilized complex emulsions displayed a dynamic morphological response to small-molecule surfactants. Some morphologies were reversible with the

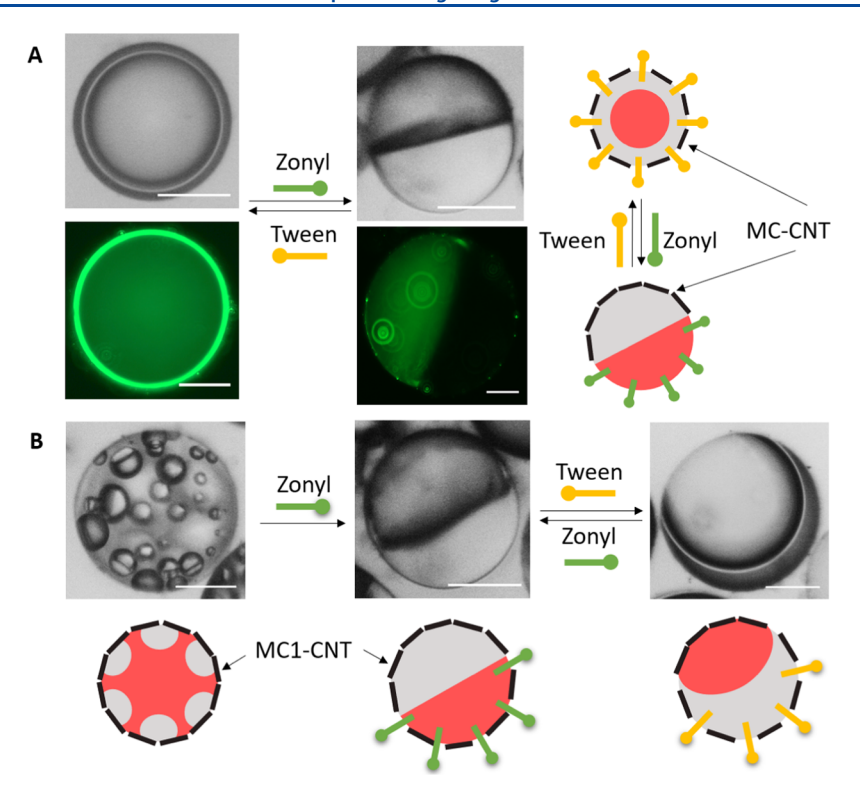


Figure 5. (A) Droplets made with 60 mg/L of MC2-CNTs. The morphology changed reversibly upon the addition of Tween or Zonyl. Fluorescence images confirm that the MC2-CNT surfactants are located at the water interface. (B) Droplets made with 60 mg/L of MC1-CNTs and 1 mg/mL of F-PBI and images showing how the morphology changes upon adding Zonyl and Tween. Scale bar = 50  $\mu$ m.

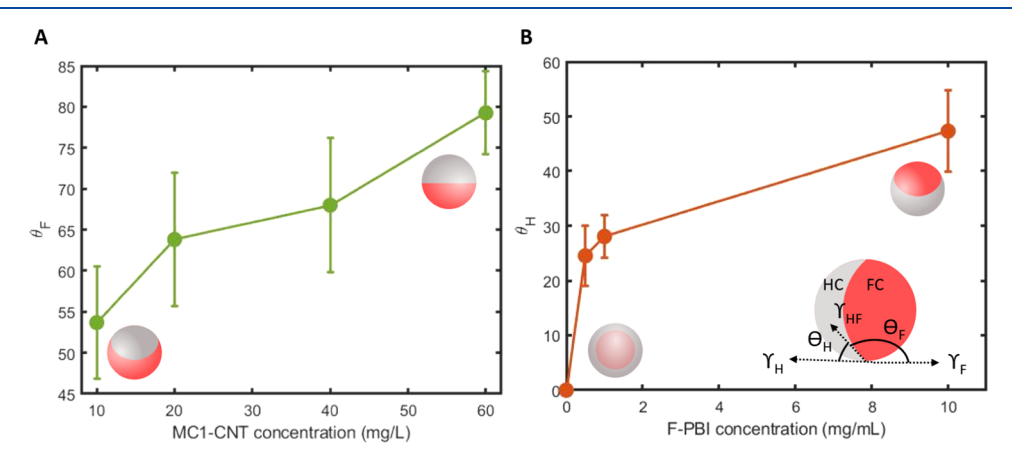


Figure 6. (A) Plot of contact angles  $\Theta_F$  between the FC-W and FC-HC interfaces versus MC1-CNT concentration, with a constant Zonyl concentration of 1 wt % and F-PBI concentration of 10 mg/mL. (B) Plot of contact angles  $\Theta_H$  between the HC-W and FC-H interfaces versus F-PBI concentration with a constant concentration of Tween at 1 wt % and a MC1-CNT concentration of 60 mg/L.

addition of Zonyl and Tween. However, CNTs bound to the droplet interfaces showed strong resistance to morphology changes even with the addition of excess Tween and Zonyl. This was explained by the strong adsorption of CNTs at the interface to form a rigid network. We foresee our MC-CNT-stabilized complex droplets to have utility in sensing and coating methods.

#### **■ EXPERIMENTAL SECTION**

**Material Synthesis.** Commercial reagents were purchased from Sigma-Aldrich and used as received without purification. The synthesis of 3,5-dinitrophenyldiazonium tetrafluoroborate is based on a previously reported method.<sup>31</sup> In this procedure, 10 g of 3,5-dinitroaniline was dissolved in 20.4 mL of water and 20 mL of tetrafluoroboric acid. The dispersion was kept at 0 °C by an ice bath

and then 3.77g of sodium nitrite in 8.2 mL of water was added dropwise to the dispersion. The mixture was stirred at 0  $^{\circ}$ C for 30 min and the resulting solid precipitate was filtered and washed with diethyl ether. The crude product was dissolved in a minimum amount of acetone and then recrystallized from diethyl ether. The final product was filtered and washed with diethyl ether three times, then dissolved in deuterated acetonitrile and characterized by  $^{1}$ H NMR spectroscopy to confirm its purity.

Figure 1A outlines the synthesis strategy of the functionalized CNTs.  $^{32}$  Pristine single-walled CNTs (p-SWCNTs) were purchased from Nano-C. p-SWCNTs weighing 10.8 mg were dispersed in 1.2 wt % Triton X-100 solution with a tip sonicator (Qsonica) at 50% amplitude for 10 min. Then, 3,5-dinitrophenyldiazonium tetrafluor-oborate measuring 1.02 g was added, followed by sparging with argon gas for 10 min and stirring at 60 °C overnight. The resulting CNTs were collected on a Teflon filter with 0.2  $\mu$ m pore size and

subsequently washed with acetone, dimethylformamide (DMF), and 1,2-dichlorobenzene (oDCB) (three times for each solvent) to remove the byproducts.

Fluorofluorescent perylene bisimide (F-PBI) synthesis was done according to Yoshinaga et al.  $^{29}$  5(6)-Carboxytetramethylrhodamine N-succinimidyl ester (RhB-NHS) was similarly prepared as described in a previous report.  $^{33}$  For the synthesis of poly(allylamine) labeled with rhodamine B (PAA-RB), 36.3 mg of poly(allylamine hydrochloride) ( $M_{\rm W}\sim17\,500$  kDa), 33  $\mu{\rm L}$  of N-ethyldiisopropylamine, and 20 mg of RhB-NHS were added to 5 mL of water. The mixture was stirred at room temperature overnight. The product was precipitated with the addition of acetone to the reaction mixture. The crude product was collected by centrifugation and washed with acetone and dichloromethane. The final product was dissolved in deuterated water and its structure was confirmed by  $^1{\rm H}$  NMR spectroscopy.

Material Characterization. Raman spectroscopy was performed using a Horiba Jobin-Yvon LabRam (Model HR 800) with 532 nm laser excitation and 1.2  $\mu$ m spot size. Samples for analysis were produced from CNT dispersions in DMF by drop casting on silicon wafers and dried in vacuum for Raman measurements. The Raman spectra from six spots were recorded for each sample. The spectra were normalized to the G-bands. The same sample was used for scanning electron microscopy (SEM), performed on a Zeiss Sigma 500 VP. X-ray photoelectron spectroscopy (XPS) was performed using a Thermo Scientific K-Alpha+ XPS. Attenuated total reflectance-Fourier transform infrared (ATR-FTIR) spectra were recorded using a Thermo Scientific Nicolet 6700 FTIR with Ge crystal.

**Droplet Fabrication.** CNT dispersions were prepared by dispersing DNB-CNTs in a 2 M aqueous solution of hexamethylenediamine (HMDA) with a tip sonicator at 50% amplitude for 10 min in an ice bath. The dispersion was sonicated for another 1 min without an ice bath to increase the temperature of the dispersion for double-emulsion fabrication.

Single emulsions were prepared by adding 50  $\mu$ L of hydrocarbon (HC) oil diethylbenzene (DEB) or fluorocarbon (FC) oil HFE7500 in 1 mL of the aqueous CNT dispersion and vortexing the mixture. Double emulsions were prepared by adding 50  $\mu$ L of the mixture of 1:1 ratio by volume of HC and FC to 1 mL of different concentrations of CNTs in aqueous dispersion and vortexing the mixture. The oil mixture was heated above the  $T_c$  so that HC and FC oils were a single homogeneous phase when added to the CNT dispersion. F-PBI was added to the FC oil at different concentrations before mixing with the HC.

**Droplet Characterization.** Top-view droplet micrographs were taken with a Leica DMRXP microscope. Side-view images were taken with a custom-built horizontal microscope consisting of an Olympus 20× objective (NA = 0.5), a Thorlabs tube lens (effective focal length = 200 mm), and an Allied Vision Prosilica GT camera.

#### ASSOCIATED CONTENT

#### Supporting Information

The Supporting Information is available free of charge at https://pubs.acs.org/doi/10.1021/acs.langmuir.1c00904.

Materials and characterization techniques; droplets micrographs and characterizations (PDF)

#### AUTHOR INFORMATION

#### **Corresponding Author**

Timothy M. Swager — Department of Chemistry, Massachusetts Institute of Technology, Cambridge, Massachusetts 02139, United States; oorcid.org/0000-0002-3577-0510; Email: tswager@mit.edu

#### **Authors**

Quynh P. Ngo – Department of Chemistry, Massachusetts Institute of Technology, Cambridge, Massachusetts 02139, United States; Department of Materials Science and Engineering, Massachusetts Institute of Technology, Cambridge, Massachusetts 02139, United States

Maggie He — Department of Chemistry, Massachusetts
Institute of Technology, Cambridge, Massachusetts 02139,
United States; Department of Chemistry and Biochemistry,
University of Arkansas, Fayetteville, Arkansas 72701, United
States; orcid.org/0000-0002-0588-9545

Alberto Concellón – Department of Chemistry, Massachusetts Institute of Technology, Cambridge, Massachusetts 02139, United States; orcid.org/0000-0002-8932-9085

Kosuke Yoshinaga — Department of Chemistry, Massachusetts Institute of Technology, Cambridge, Massachusetts 02139, United States

Shao-Xiong Lennon Luo — Department of Chemistry, Massachusetts Institute of Technology, Cambridge, Massachusetts 02139, United States; orcid.org/0000-0001-5308-4576

Nouf Aljabri — Department of Chemistry, Massachusetts Institute of Technology, Cambridge, Massachusetts 02139, United States; Exploration Advanced Research Center (EXPEC ARC), Saudi Aramco, Dhahran 31311, Saudi Arabia

Complete contact information is available at: https://pubs.acs.org/10.1021/acs.langmuir.1c00904

#### Notes

The authors declare no competing financial interest.

### ACKNOWLEDGMENTS

This work was supported by the National Science Foundation DMR-1809740. The authors thank their colleagues in Swager Group for their insightful discussions and suggestions, especially Dr. Harikrishnan Vijayamohanan (MIT) and Dr. Kanghee Ku (MIT). K.Y. thanks Funai Overseas Scholarship for financial support.

## REFERENCES

- (1) Berton-Carabin, C. C.; Schroën, K. Pickering Emulsions for Food Applications: Background, Trends, and Challenges. *Annu. Rev. Food Sci. Technol.* **2015**, *6*, 263–297.
- (2) Marto, J.; Nunes, A.; Martins, A. M.; Carvalheira, J.; Prazeres, P.; Gonçalves, L.; Marques, A.; Lucas, A.; Ribeiro, H. M. Pickering Emulsions Stabilized by Calcium Carbonate Particles: A New Topical Formulation. *Cosmetics* **2020**, *7*, No. 62.
- (3) Albert, C.; Beladjine, M.; Tsapis, N.; Fattal, E.; Agnely, F.; Huang, N. Pickering Emulsions: Preparation Processes, Key Parameters Governing Their Properties and Potential for Pharmaceutical Applications. *J. Controlled Release* **2019**, 302–332.
- (4) Tarimala, S.; Ranabothu, S. R.; Vernetti, J. P.; Dai, L. L. Mobility and in Situ Aggregation of Charged Microparticles at Oil–Water Interfaces. *Langmuir* **2004**, *20*, 5171–5173.
- (5) Binks, B. P.; Fletcher, P. D. I. Particles Adsorbed at the Oil—Water Interface: A Theoretical Comparison between Spheres of Uniform Wettability and "Janus" Particles. *Langmuir* **2001**, *17*, 4708—4710.
- (6) Zeininger, L.; Nagelberg, S.; Harvey, K. S.; Savagatrup, S.; Herbert, M. B.; Yoshinaga, K.; Capobianco, J. A.; Kolle, M.; Swager, T. M. Rapid Detection of Salmonella Enterica via Directional Emission from Carbohydrate-Functionalized Dynamic Double Emulsions. ACS Cent. Sci. 2019, 5, 789–795.

- (7) Zentner, C. A.; Anson, F.; Thayumanavan, S.; Swager, T. M. Dynamic Imine Chemistry at Complex Double Emulsion Interfaces. *J. Am. Chem. Soc.* **2019**, *141*, 18048–18055.
- (8) Li, J.; Savagatrup, S.; Nelson, Z.; Yoshinaga, K.; Swager, T. M. Fluorescent Janus Emulsions for Biosensing of Listeria Monocytogenes. *Proc. Natl. Acad. Sci. U.S.A.* **2020**, *117*, 11923–11930.
- (9) Nagelberg, S.; Zarzar, L. D.; Nicolas, N.; Subramanian, K.; Kalow, J. A.; Sresht, V.; Blankschtein, D.; Barbastathis, G.; Kreysing, M.; Swager, T. M.; Kolle, M. Reconfigurable and Responsive Droplet-Based Compound Micro-Lenses. *Nat. Commun.* **2017**, *8*, No. 14673.
- (10) Ku, K. H.; Li, J.; Yoshinaga, K.; Swager, T. M. Dynamically Reconfigurable, Multifunctional Emulsions with Controllable Structure and Movement. *Adv. Mater.* **2019**, *31*, No. 1905569.
- (11) Briggs, N.; Raman, A. K. Y.; Barrett, L.; Brown, C.; Li, B.; Leavitt, D.; Aichele, C. P.; Crossley, S. Stable Pickering Emulsions Using Multi-Walled Carbon Nanotubes of Varying Wettability. *Colloids Surf., A* **2018**, *537*, 227–235.
- (12) Briggs, N. M.; Weston, J. S.; Li, B.; Venkataramani, D.; Aichele, C. P.; Harwell, J. H.; Crossley, S. P. Multiwalled Carbon Nanotubes at the Interface of Pickering Emulsions. *Langmuir* **2015**, *31*, 13077–13084
- (13) Wang, H.; Hobbie, E. K. Amphiphobic Carbon Nanotubes as Macroemulsion Surfactants. *Langmuir* **2003**, *19*, 3091–3093.
- (14) Kim, J.; Cote, L. J.; Kim, F.; Yuan, W.; Shull, K. R.; Huang, J. Graphene Oxide Sheets at Interfaces. J. Am. Chem. Soc. 2010, 132, 8180–8186.
- (15) Hrapovic, S.; Liu, Y.; Male, K. B.; Luong, J. H. T. Electrochemical Biosensing Platforms Using Platinum Nanoparticles and Carbon Nanotubes. *Anal. Chem.* **2004**, *76*, 1083–1088.
- (16) Chen, W.; Liu, X.; Liu, Y.; Kim, H. Il Novel Synthesis of Self-Assembled CNT Microcapsules by O/W Pickering Emulsions. *Mater. Lett.* **2010**, *64*, 2589–2592.
- (17) Wang, W.; Laird, E. D.; Gogotsi, Y.; Li, C. Y. Bending Single-Walled Carbon Nanotubes into Nanorings Using a Pickering Emulsion-Based Process. *Carbon* **2012**, *50*, 1769–1775.
- (18) Strauss, M. J. Anionic Sigma Complexes. Chem. Rev. 1970, 70, 667–712.
- (19) Terrier, F. Rate and Equilibrium Studies in Jackson-Meisenheimer Complexes. *Chem. Rev.* **1982**, *82*, *77*–152.
- (20) Proctor, J. E.; Armanda, D. A. M.; Vijayaraghavan, A. An Introduction to Graphene and Carbon Nanotubes; CRC Press, Taylor & Francis Group: Boca Raton, FL, 2017.
- (21) Jeon, I.; Yoon, B.; He, M.; Swager, T. M. Hyperstage Graphite: Electrochemical Synthesis and Spontaneous Reactive Exfoliation. *Adv. Mater.* **2018**, *30*, No. 1704538.
- (22) Bisswanger, H. Multiple Equilibria, Principles, and Derivations. In *Enzyme Kinetics*; Wiley-VCH Verlag GmbH & Co. KGaA: Weinheim, Germany, 2017; pp 1–26.
- (23) Wu, T.; Wang, H.; Jing, B.; Liu, F.; Burns, P. C.; Na, C. Multi-Body Coalescence in Pickering Emulsions. *Nat. Commun.* **2015**, *6*, No. 5929
- (24) Backes, C.; Hauke, F.; Hirsch, A. The Potential of Perylene Bisimide Derivatives for the Solubilization of Carbon Nanotubes and Graphene. *Adv. Mater.* **2011**, 23, 2588–2601.
- (25) Tournus, F.; Latil, S.; Heggie, M. I.; Charlier, J. C.  $\pi$ -Stacking Interaction between Carbon Nanotubes and Organic Molecules. *Phys. Rev. B* **2005**, 72, No. 075431.
- (26) Backes, C.; Mundloch, U.; Schmidt, C. D.; Coleman, J. N.; Wohlleben, W.; Hauke, F.; Hirsch, A. Enhanced Adsorption Affinity of Anionic Perylene-Based Surfactants towards Smaller-Diameter SWCNTs. *Chem. Eur. J.* **2010**, *16*, 13185–13192.
- (27) Backes, C.; Hauke, F.; Hirsch, A. Tuning the Adsorption of Perylene-Based Surfactants on the Surface of Single-Walled Carbon Nanotubes. *Phys. Status Solidi B* **2013**, 250, 2592–2598.
- (28) Manzetti, S.; Gabriel, J.-C. P. Methods for Dispersing Carbon Nanotubes for Nanotechnology Applications: Liquid Nanocrystals, Suspensions, Polyelectrolytes, Colloids and Organization Control. *Int. Nano Lett.* **2019**, *9*, 31–49.

- (29) Yoshinaga, K.; Swager, T. M. Fluorofluorescent Perylene Bisimides. *Synlett* **2018**, *29*, 2509–2514.
- (30) Concellón, A.; Zentner, C. A.; Swager, T. M. Dynamic Complex Liquid Crystal Emulsions. J. Am. Chem. Soc. 2019, 141, 18246–18255.
- (31) Hanson, P.; Jones, J. R.; Taylor, A. B.; Walton, P. H.; Timms, A. W. Sandmeyer reactions. Part 7.1 An investigation into the reduction steps of Sandmeyer hydroxylation and chlorination reactions. *J. Chem. Soc., Perkin Trans.* 2 2002, 6, 1135–1150.
- (32) Dyke, C. A.; Stewart, M. P.; Maya, F.; Tour, J. M. Diazonium-Based Functionalization of Carbon Nanotubes: XPS and GC-MS Analysis and Mechanistic Implications. *Synlett* **2004**, 2004, 155–160.
- (33) Gential, G. P. P.; et al. Synthesis and evaluation of fluorescent Pam3Cys peptide conjugates. *Bioorg. Med. Chem. Lett.* **2016**, 26, 3641–3645.